Optically interrogated MEMS pressure sensors for propulsion applications

Jie Zhou
Department of Electrical and Computer Engineering and Computer Science
University of Cincinnati
Cincinnati, Ohio 45221-0030

Samhita Dasgupta
Taitech, Inc.
AMC P.O. Box 33630
WPAFB, Ohio 45433-0630

Hiroshi Kobayashi
J. Mitch Wolff
Department of Mechanical and Materials Engineering
Wright State University
Dayton, Ohio 45435-0001

Howard E. Jackson
Department of Physics
University of Cincinnati
Cincinnati, Ohio 45221-0011

Joseph T. Boyd
Department of Electrical and Computer Engineering and Computer Science
University of Cincinnati
Cincinnati, Ohio 45221-0030
E-mail: jboyd@ececs.uc.edu

Abstract. Pressure sensors suitable for propulsion applications that utilize interrogation by fiber optics are described. To be suitable for many propulsion applications, sensors should have fast response, have a configuration that can be readily incorporated into sensor arrays, and be able to survive harsh environments. Microelectromechanical systems (MEMS) technology is utilized here for sensor fabrication. Optically interrogated MEMS devices are expected to eventually be more suitable than electrically interrogated MEMS devices for many propulsion applications involving harsh environments. Pressure-sensor elements are formed by etching shallow cavities in glass substrates followed by anodic bonding of silicon onto the glass over the cavity. The silicon is subsequently etched to form the pressure-sensitive diaphragm. Light emerging from a fiber is then used to interferometrically detect diaphragm deflection due to external pressure. Experimental results for static and dynamic pressure tests carried out in a shock tube demonstrate reasonable linearity, sensitivity, and time response. [DOI: 10.1117/1.1354629]

Subject terms: MEMS; fiber sensors; propulsion.

Paper 200204 received May 23, 2000; revised manuscript received Oct. 17, 2000; accepted for publication Oct. 17, 2000.

1 Introduction

Microelectromechanical systems (MEMS) technology is effective for fabricating pressure sensors because the small and definite size of the sensing elements results in the desirable properties of large bandwidth and high sensitivity. Optical interrogation of these sensing elements is advantageous because (1) it is expected to be far superior to electrical interrogation in harsh environments, (2) multiple sensors, such as in an array, can use wavelength division multiplexing (WDM), which may be simpler and more effective than using electronic interrogation, and (3) optical fibers can connect sensor arrays to electronics, so that all electronics can be removed from harsh environments. In this paper we consider pressure sensors utilizing MEMS technology for sensor fabrication and interrogation by light propagating in optical fibers. We anticipate that these sensors will be applicable for propulsion applications, because their structure can readily be incorporated into arrays, they provide sufficiently fast response, and they have survived harsh environments.

Optical fiber sensors can have a large variety of configurations.[1] Optical pressure sensors of the type we are considering have been reported in a variety of configurations, such as those using modulation of the air gap of a Fabry-Perot interferometer by deflection of a diaphragm,[2–4] photoelastic modulation of polarization state,[5] interferometric detection of the stress-dependent resonant frequency of an optically excited vibrating beam,[6,7] and mechanical coupling of a diaphragm and integrated optical interferometer to produce photoelastic modulation of the interferometer optical-path-length difference.[8–12] Here we use a silicon diaphragm anodically bonded to a glass substrate with a cavity previously etched into it. The surface of the silicon diaphragm and the glass-air interface form reflectors for the Fabry-Perot cavity. This configuration is very rugged and, with the sturdy packaging we utilize to hold the sensing element and the fiber delivering light to the Fabry-Perot cavity, allows our configuration to both survive and maintain operation in a simulated propulsion environment such as an experimental shock tube. Previously there has been some work involving optical fiber sensors being utilized to characterize engine and wind-tunnel environments.[13–15]

In what follows we present a detailed design of the sensor-element configuration, details of the fabrication and packaging of the sensor element and optical fiber, a description of the optical detection scheme, and both static and dynamic experimental results, the latter obtained in a shock tube.

 0091-3286/2001/$15.00

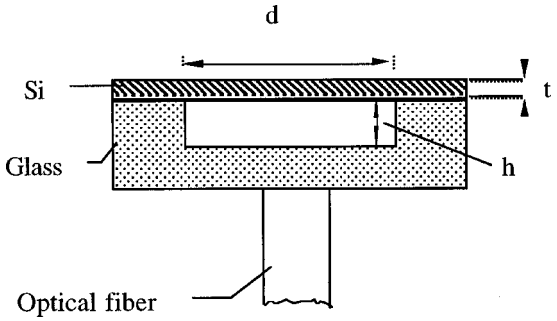

Fig. 1 Configuration of the optically interrogated MEMS pressure sensor with $d=2R_0$.

2 Sensor and Package Design

The configuration of the individual MEMS–optical-fiber pressure sensor consists of a glass plate with a shallow cylindrical cavity etched into one surface and a thin silicon diaphragm that covers the cavity, as shown schematically in Fig. 1. In Fig. 1 the position of the diaphragm deflects in response to pressure. A hole from the bottom of the plate to the cavity can be included if a relative-pressure sensor is needed. When we have included such a hole, it has been convenient to connect it to a second cylindrical cavity that has a small connection to the pressure-sensing cavity. Light is introduced into the pressure-sensing cavity from an optical fiber through the glass and propagates perpendicular to the diaphragm-cavity interface (Fig. 1). The silicon-diaphragm–cavity interface reflects most of the light, and the cavity-glass interface acts as the second reflector, thus forming a Fabry-Perot interferometer. Pressure causing the thin Si diaphragm to move changes the separation between reflectors. This change in separation results in a different amount of light reflected, and thus measurement of this change of reflected light can be related to pressure. The key design parameters of diaphragm thickness, initial cavity depth, and cavity diameter can be varied to provide linear response over various pressure ranges. Our design software allows us to tune the pressure range and frequency response appropriately for several applications.

In the configuration shown in Fig. 1, reflected light, after multiple reflections within the cavity, is carried back through the same fiber. The reflectance R is given by[16]

$$R=\left|r_1^+ + \frac{t_1^+ t_1^- r_2^+ e^{i\phi}}{1-r_1^+ r_2^+ e^{i\phi}}\right|^2, \tag{1}$$

where

$$r_1^+ = \frac{n_{\text{glass}}-1}{n_{\text{glass}}+1}, \tag{2a}$$

$$t_1^- = \frac{2}{n_{\text{glass}}+1}, \tag{2b}$$

$$r_2^+ = -\frac{n_{\text{silicon}}-1}{n_{\text{silicon}}+1}, \tag{2c}$$

$$t_1^+ = \frac{2n_{\text{glass}}}{n_{\text{glass}}+1}, \tag{2d}$$

and

$$\phi = 2\pi(2h)/\lambda_0. \tag{2e}$$

As seen from Eq. (1), the reflected light intensity varies periodically as a function of the cavity depth h. The sensitivity is controlled mainly by choosing the diaphragm thickness, as this thickness determines how much deflection results from a given amount of pressure. As noted earlier, deflection corresponds to a cavity length change and hence a change in reflected light intensity.

We modeled the top diaphragm surface as a circular membrane. The deflection of the diaphragm due to the application of pressure P is thus given by[17,18]

$$w_r = w_c\left[1-\left(\frac{r}{R_0}\right)^2\right]^2 = \frac{3PR_0^4(1-\gamma^2)}{16Et^3}\left[1-\left(\frac{r}{R_0}\right)^2\right]^2, \tag{3}$$

where r is the distance from the center of the plate, w_r is the deflection at r, w_c is the deflection at $r=0$, P is the normal pressure, R_0 is the radius of the diaphragm, γ is Poisson's ratio for silicon, E is Young's modulus, and t is the diaphragm thickness. To avoid ambiguities, the maximum diaphragm deflection is typically restricted to values corresponding to a single value of light intensity, that is, a deflection of $\lambda_0/4$, where λ_0 is the operating wavelength. However, we wish to design the cavity so that at zero pressure or zero diaphragm deflection, the reflectance R in Eq. (1) takes on the average value of its sinusoidal variation. This ensures optimum linearity in pressure response, but for a positive pressure range, the maximum deflection was restricted to $\lambda_0/8$ to provide a single-valued relation between reflected light intensity and pressure. Thus, the pressure that causes a deflection of $\lambda_0/8$ is given by

$$P = \frac{2Et^3\lambda_0}{3R_0^4(1-\gamma^2)}. \tag{4}$$

As can be seen from the above equation, the thickness and the diameter of the diaphragm are crucial parameters for sensor design. A maximum deflection of $\lambda_0/4$ could be chosen for positive pressure ranges only, thus increasing the range of nearly linear response.

We initially designed pressure sensors to respond over the pressure range 0 to 30 psi, to operate at $\lambda_0=850$ nm, and chose $R_0=300\,\mu$m as a size compatible with testing and fabrication. For this maximum pressure and diaphragm radius, Eq. (4) implies that the diaphragm thickness of $t=26.2\,\mu$m will provide $\lambda_0/8$ deflection at the maximum pressure. We thus fabricated a diaphragm having thickness close to this value.

There are several constraints in choosing the depth of the etched cavity in the glass wafer. First, it must be greater than the maximum diaphragm deflection $\lambda_0/8$. To avoid ambiguities that could arise through use of a broadband light source, it should be sufficiently small to yield a cavity free spectral range[19] somewhat greater than the LED line-

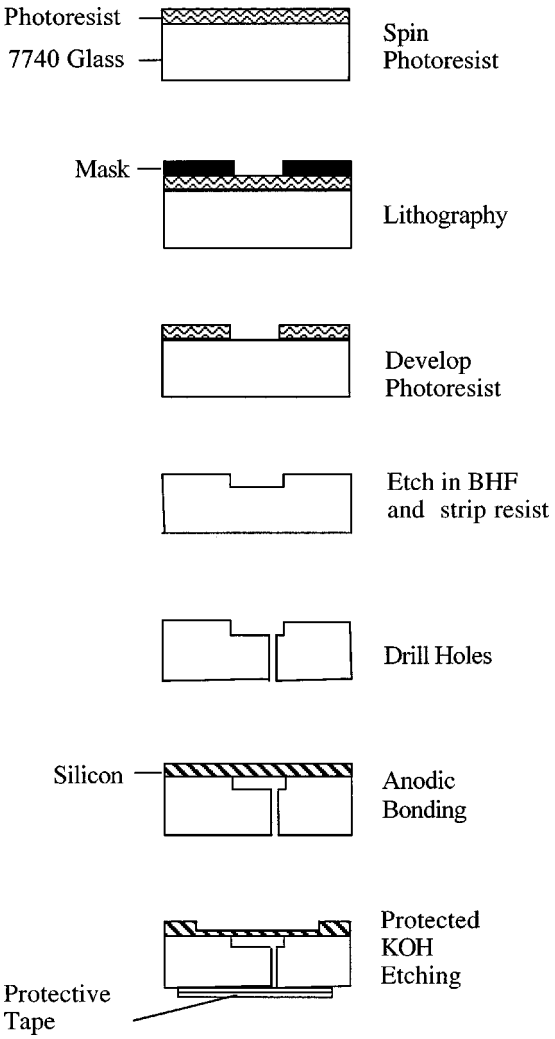

Fig. 2 Processing steps for fabrication of the optically interrogated MEMS pressure sensor.

width of 100 nm. A free spectral range of 100 nm corresponds to a cavity depth of $\approx 4\ \mu$m, so we are able to choose a value smaller than this, but not so small as to reduce the pressure sensitivity. Also, we chose the cavity depth to be somewhat larger than $\lambda_0/8$ to avoid the possibility of the diaphragm bonding to the bottom of the cavity during fabrication. Finally, we wish the zero-deflection point to correspond to the mean value of the reflectance R in order to provide maximum linearity; we thus chose $h = 0.53\ \mu$m.

3 Fabrication of Sensor Elements and Packaging

Microfabrication methods were used to fabricate the pressure-sensor elements. Figure 2 shows the processing steps used during the fabrication process. The process was initiated with a standard fused-silica wafer polished on both sides that was patterned to form a series of cavities for the Fabry-Perot interferometer. Standard photolithographic and etching techniques were used for this process. A silicon wafer polished on both sides was then electrostatically bonded to the patterned glass wafer. Bulk etching techniques were then used to thin the silicon wafer down to the desired diaphragm thickness. Finally, for initial evaluation, the sensors were separated using a standard dicing saw.

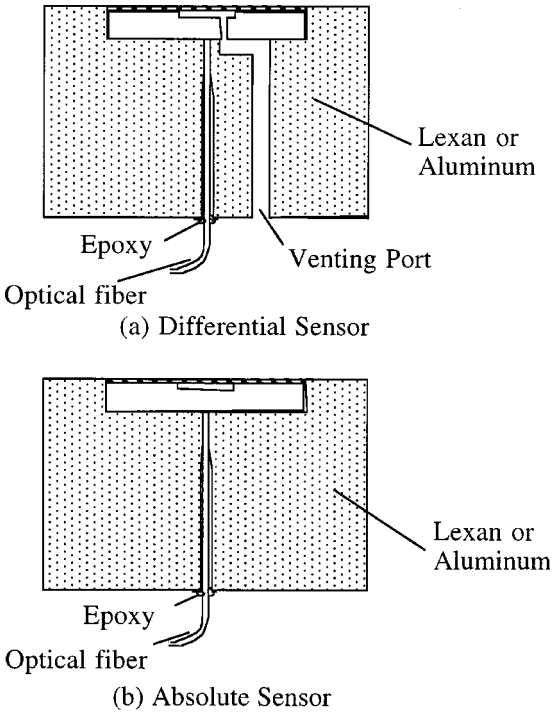

Fig. 3 Package configurations for housing the optical fiber and MEMS pressure sensor: (a) differential pressure sensor, (b) absolute pressure sensor.

The glass-diaphragm structure and the fiber are mounted in a sturdy Lexan or aluminum package, which is able to maintain their proximity to each other in the presence of harsh external environments. Figure 3 shows the package configuration for both a differential and an absolute sensor configuration. The packaged sensors were then placed on a mounting assembly suitable for static and dynamic testing.

4 Optical Detection Scheme

A broadband light-emitting diode (LED) centered at 850 nm was used as the illumination source for the sensor. Because reflectivity is a function of wavelength and changes with pressure, the reflected light from the sensor appears to be spectrally shifted by external pressure. A ratio signal from the two detectors was used to detect the spectral shift, as shown in Fig. 4. The light was routed to the sensor through a 2×2 coupler. The reflected light was collected back through the same fiber and routed to a second 2×2

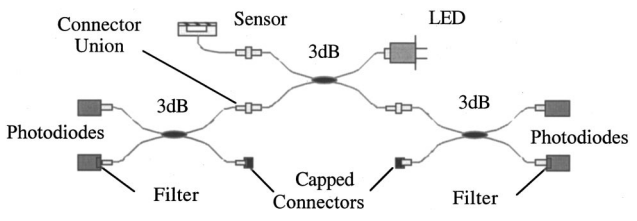

Fig. 4 Electro-optic system for interrogating fiber-coupled MEMS pressure sensors.

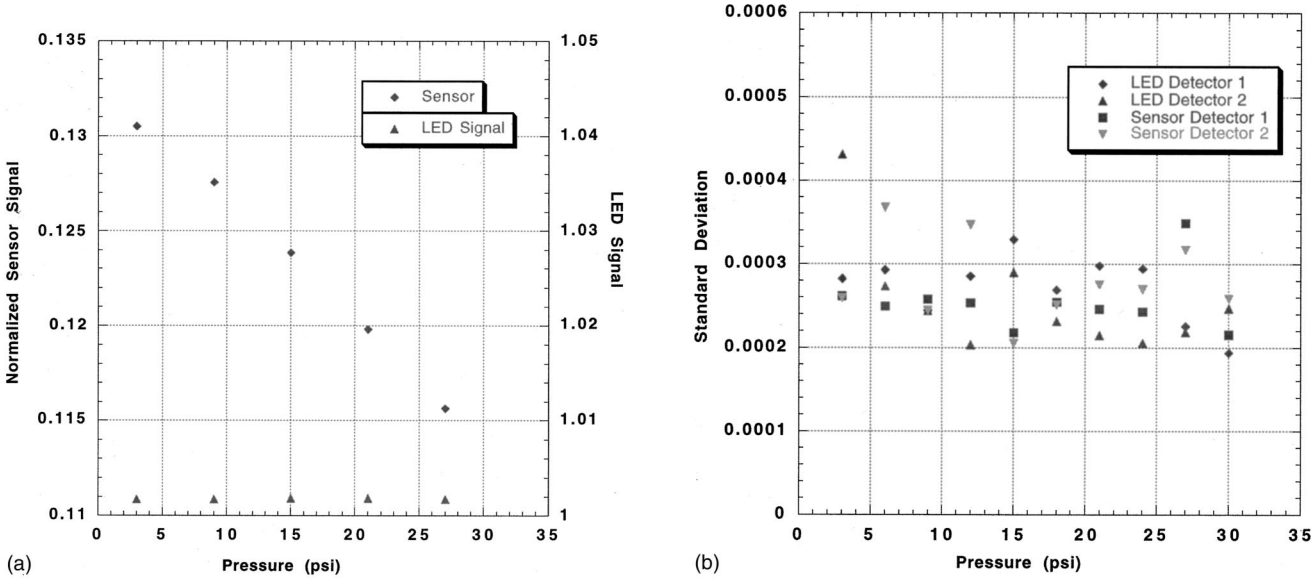

Fig. 5 (a) Static response of an optically interrogated MEMS pressure sensor in which normalized sensor signal is plotted as a function of pressure; (b) standard deviation of the signal at various detectors in the electro-optic interrogation system.

coupler that was used to split the reflected light into equal-intensity portions. One portion of the divided signal was terminated onto a photodetector, and the other was terminated onto a broadband bandpass optical filter and a photodiode combination. The ratio of the outputs of the two photodetectors was used as the measure for the sensed parameter. The sensor output is measured by the ratio of V_{S1} and V_{S2}, where V_{S1} is the output of the photodetector with the bandpass filter and V_{S2} is the output of the second photodetector with no filter. The output of the LED is monitored using the ratio of the outputs from a similar pair of photodetectors, V_{L1} and V_{L2}. In this paper, the sensor signal thus is the ratio V_{S1}/V_{S2} and the LED signal is the ratio V_{L1}/V_{L2}. Use of the ratio causes many variations and drift effects to divide out of the final result. Currently the division is performed in software, but the incorporation of an analog divider into the detection circuitry is currently in progress. Detailed analytical evaluation of this detection configuration indicates that the ratio signal can provide a linear response to pressure over a substantial range for practical sensor parameters.

A key element in this detection method was the ability to ensure integrity of output characteristics for the LED and the photodiodes. Small changes in environmental conditions can cause changes in the output similar in magnitude to those produced by the change in pressure on the Fabry-Perot cavity. The LED and photodiodes were maintained at a constant temperature with a thermoelectric cooler assembly that is continuously monitored. A multimode 100–140-μm fiber was used for the light connections to and from the sensor.

5 Experimental Results

Fabricated absolute-pressure sensors were tested under a variety of operating conditions. These sensors were fabricated with $h=0.53\,\mu$m, $R_0=300\,\mu$m, and $t=26.2\,\mu$m. Initial tests of the sensors were detailed calibration runs over a pressure range of 0.5 to 30 psi, since the sensors were designed for a full-scale reading of 30 psi. The output from the photodetectors connected to the sensor and the LED were recorded with a computer-based data acquisition system as a function of pressure. The pressure was also monitored with a pressure calibrator. One hundred samples were taken at each pressure value. Figure 5(a) shows a plot of the sensor signal as a function of pressure, each point being an average of the 100 readings acquired. The data show a steady, monotonic, nearly linear variation with pressure, whereas the LED signal remains constant, as expected. The sensor sensitivity corresponding to the photodiode signal voltage associated with the data in Fig. 5(a) is 1.77 mV/psi, a value within a factor of 2 of what is estimated from the design and the power level utilized. Similar data acquisitions were performed over several cycles to ensure no drift occurred in the readings. Figure 5(b) shows a plot of the standard deviation for each of the detector outputs divided by the mean. As seen from this plot, the scatter in the data was less than 0.25%.

The individual pressure sensor was then tested for its dynamic response in a shock-tube facility. Figure 6 shows a schematic of the shock tube facility at Wright State University that was used to perform the testing. This facility is designed for dynamic calibration of pressure transducers for turbomachinery applications.[20] The shock tube was utilized to generate a total pressure rise at the sensor of 10.6 psi according to 1D compressible-flow theory. The rise time is estimated to be about 10 ns, based on measurements characterizing a similar system.[21] A total of five separate runs were used; the frequency-domain results presented here correspond to the transfer function observed.

Figure 7(a) shows a typical time trace of the response of the detector due to the shock wave. A sharp response to the shock-wave pressure rise is immediately noticeable. The sensor shows some overshoot before reaching a constant

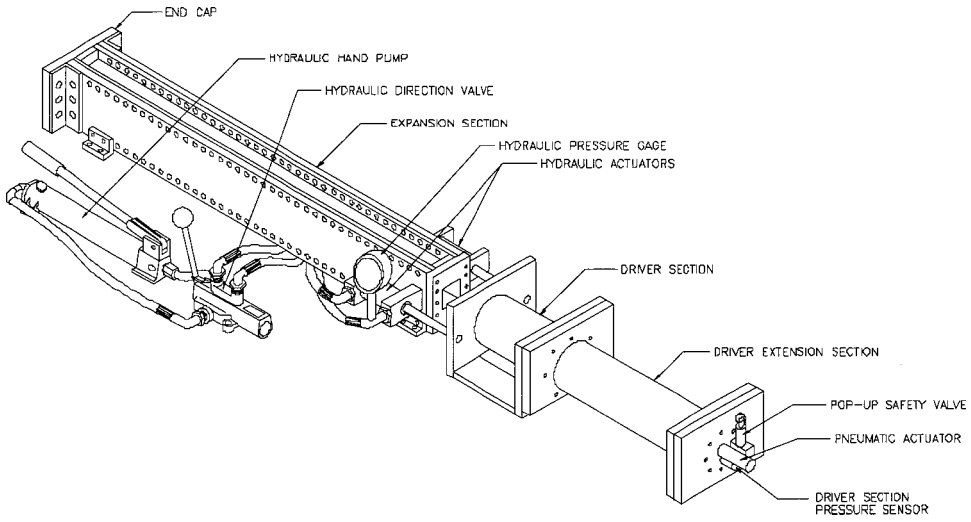

Fig. 6 Schematic diagram of the shock-tube configuration.

output. The pressure step magnitude is about 10 psi, as expected from the theoretical calculation. The response before and after the shock wave is noise associated with the shock-tube system.

A frequency-response function analysis is performed by taking the cross spectral density function of the input to output and the auto spectral density function of the input. The number of data used in the analysis is 4096, and the frequency resolution increment is 1.22 kHz. The response of the sensor and the ideal step inputs are weighted with an exponential window to suppress the leakage of frequency spectrum due to taking an incomplete cycle. Figure 7(b) shows a plot of the average frequency response. The plotted line shows the averaged response from multiple samples. A high peak at 140 kHz was apparent in the results.

During the sensor design phase, calculations of the frequency response characteristics were performed, based on a vibrating circular diaphragm. These calculations were based on the mechanical properties of the diaphragm material (silicon) and the vibration characteristics of a circular flat plate. They indicated resonance frequencies in the megahertz range for the sensor, due to its small size and diaphragm thickness.

The measured response of the sensor, on the other hand, depends not only on the response characteristics of the sensor, but also on the response characteristics of the electro-optical components in the system: a LED operating in the continuous-wave mode, and silicon *pin* photodiodes coupled with amplifiers. The time-varying data were acquired by sampling the integrated photodetector-amplifier units. Thus the response of the sensor system is a combination of the sensor response and the sampled detector-amplifier response, which for components used in this work was limited to 210 kHz. Based on this limitation, we infer that the overall response of the sensor is currently limited by the detector response.

An encouraging result of these dynamic calibration tests is the usable frequency of the fabricated sensor. The flat response of the sensor extends up to 30 kHz. The response characteristics compare favorably with current and devel-

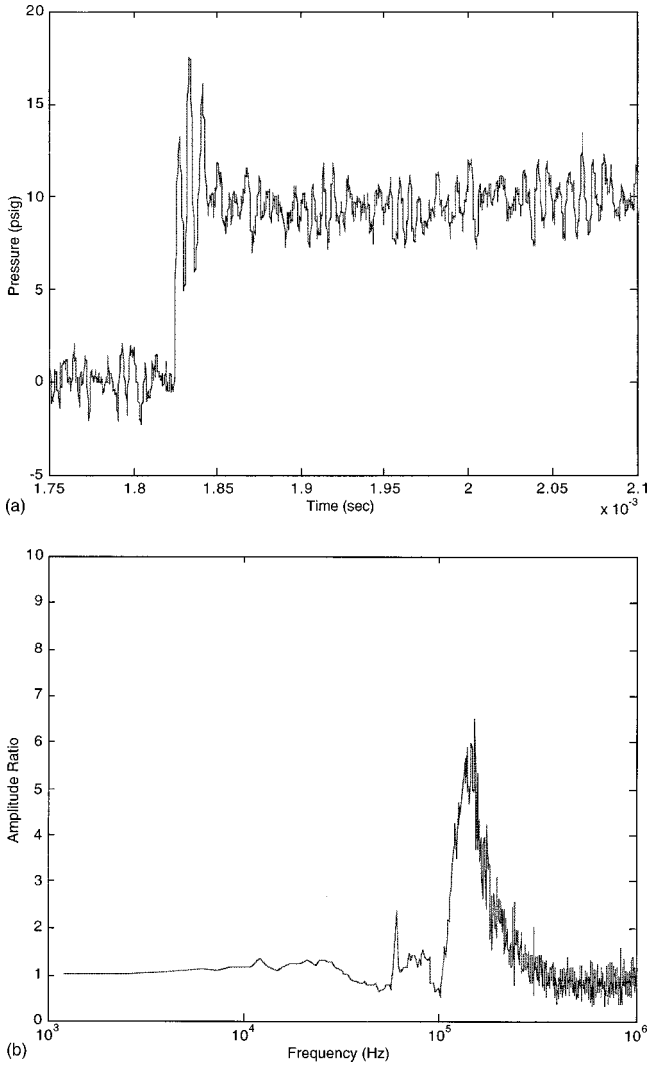

Fig. 7 (a) Typical time trace of the normal shock wave passing the sensor. (b) Transfer function of the fiber optic MEMS pressure sensor.

oping sensor technologies. Furthermore, the sensor has an adequate unsteady-pressure measurement capability for high-speed propulsion applications, such as for gas turbines.[20]

6 Summary

Pressure sensors utilizing MEMS technology for fabrication of the sensing element and interrogation by fiber optics have been described. These elements have been designed so that they can readily be incorporated into a pressure-sensor array. We have demonstrated that these optically interrogated MEMS devices survived and operated in a shock-tube environment, inferring they may be suitable for many propulsion applications involving harsh environments. Experimental results for static pressure tests and dynamic pressure tests carried out in a shock tube demonstrate pressure sensitivity close to that predicted by design, nearly linear response with respect to pressure, and fast response.

Acknowledgments

We acknowledge the assistance of William F. Terry in mounting and packaging of the sensors and the design and assembly of the sensor interface unit, and of Dr. Gregory N. De Brabander in the initial design phase. This study has been supported in part by a joint AFRL/DAGSI (Dayton Area Graduate Studies Institute) grant, AFOSR, the propulsion directorate of AFRL, and NASA. We appreciate being able to perform some testing at Wright-Patterson Air Force Base.

References

1. B. Culshaw, G. W. Day, A. D. Kersey, and Y. Ohtsuka, Eds., Special Issue on Optical Fiber Sensors, *J. Lightwave Technol.* **13**, (1995).
2. G. Beheim, K. Fritsch, and R. Poorman, ''Fiber-linked interferometric pressure sensor,'' *Rev. Sci. Instrum.* **58**, 1655–1659 (1987).
3. R. A. Wolthuis, G. L. Mitchell, E. Saaski, J. C. Hartl, and M. A. Afromowitz, ''Development of medical pressure and temperature sensors employing optical spectrum modulation,'' *IEEE Trans. Biomed. Eng.* **38**, 974–980 (1991).
4. Y. Kim and D. P. Neikirk, ''Micromachined Fabry-Perot cavity pressure transducer,'' *IEEE Photonics Technol. Lett.* **12**, 1471–1473 (1995).
5. G. Beheim and D. J. Anthan, ''Fiber-optic photoelastic pressure sensor with fiber-loss compensation,'' *Opt. Eng.* **12**, 220–222 (1987).
6. D. Angelidis and P. Parsons, ''Optical micromachined pressure sensor for aerospace applications,'' *Opt. Eng.* **31**, 1638–1641 (1992).
7. H. Unzeitig and H. Bartelt, ''All-optical pressure sensor with temperature compensation on resonant PECVD silicon nitride microstructures,'' *Electron. Lett.* **28**, 400–402 (1992).
8. M. Ohkawa, M. Izutsu, and T. Sueta, ''Integrated optic pressure sensor on silicon substrate,'' *Appl. Opt.* **28**, 5153–5157 (1989).
9. G. N. De Brabander, J. T. Boyd, and G. Beheim, ''Integrated optical ring resonator with micromechanical diaphragm for pressure sensing,'' *IEEE Photonics Technol. Lett.* **6**, 671–673 (1994).
10. A. Vadekar, A. Nathan, and W. P. Huang, ''Analysis and design of an integrated silicon ARROW Mach-Zehnder micromechanical interferometer,'' *J. Lightwave Technol.* **12**, 157–162 (1994).
11. K. Fischer, J. Müller, R. Hoffmann, F. Wasse, and D. Salle, ''Elastooptical properties of SiON layers in an integrated optical interferometer used as a pressure sensor,'' *J. Lightwave Technol.* **12**, 163–169 (1994).
12. G. N. De Brabander, G. Beheim, and J. T. Boyd, ''Integrated optical micromachined pressure sensor with spectrally encoded output and temperature compensation,'' *Appl. Opt.* **37**, 3264–3267 (1998).
13. R. A. Atkins, J. H. Gardner, W. N. Gibler, C. E. Lee, M. D. Oakland, M. O. Spears, V. P. Swenson, H. F. Taylor, J. J. McCoy, and G. Beshouri, ''Fiber-optic pressure sensors for internal combustion engines,'' *Appl. Opt.* **33**(7), 1315–1320 (1994).
14. J. Castracane and L. P. Chow, ''Optical multichannel transducer array for wind tunnel applications,'' *Opt. Eng.* **35**, 2627–2633 (1996).
15. M. Komachiya, H. Sonobe, T. Fumino, T. Sakaguchi, K. Kawakami, S. Wantanabe, and T. Sasayama, ''Knocking detection of a gasoline engine by utilizing an optical fiber with specific refractive-index composition,'' *Appl. Opt.* **37**, 1152–1158 (1998).
16. J. M. Vaughn, *The Fabry-Perot Interferometer—History, Theory, Practice, and Application*, pp. 89–97, A. Hilger (1989).
17. L. Landeau and L. Lifschitz, *Theory of Elasticity*, Pergamon (1970).
18. J. R. Vinson, *Structural Mechanics: The Behavior of Plates and Shells*, Wiley (1974).
19. M. Born and E. Wolf, *Principles of Optics*, Pergamon (1964).
20. H. Kobayashi, T. Leger, and J. M. Wolff, ''Experimental and theoretical frequency response of pressure transducers for high speed turbomachinery,''AIAA Paper 98-3745; and *Int. J. Turbo and Jet Engines* (in press).
21. E. O. Doebelin, *Measurement Systems—Application and Design*, 4th ed., p. 485, McGraw-Hill (1990).

Jie Zhou completed his BS degree in optical engineering at Huazhong University of Science and Technology, Wuhan, China, in 1984. He received his MS degree in applied physics from Beijing Polytechnic University and another one in physics from Hampton University, Hampton, Virginia, in 1988 and 1995, respectively. He is currently a PhD candidate in the Electrical and Computer Science Department, University of Cincinnati, Cincinnati, Ohio. His research interests include fiber optics, optical sensors and micro fabrication. Mr. Zhou is a member of OSA and SPIE.

Samhita Dasgupta earned her PhD from the University of Cincinnati in 1986. Following her graduation, she was a member of the optical computing group at the University of California, San Diego, where she performed research on the development of 2D spatial light modulator devices. From 1989 to 1993, Dr. Dasgupta was a member of the Advanced Controls Technology Group at GE Aircraft Engines in Cincinnati, Ohio. Currently she is a senior research scientist at Taitech, Inc., and a research assistant professor at the University of Cincinnati. Her current research includes micro-optomechanical (MEMS/MOEMS) sensors and optical diagnostics for aerospace applications. She is an associate fellow of AIAA and the chair of the AIAA Sensor Systems Technical Committee.

Hiroshi Kobayashi received his BS and MS degrees in mechanical engineering from Wright State University in 1997 and 1999, respectively. His MS thesis was entitled ''Unsteady Pressure Measurement Issues for High Speed Turbomachinery Applications.'' He is currently a mechanical design engineer for Tokyo Electron Yamanashi Ltd., in Nagano, Japan.

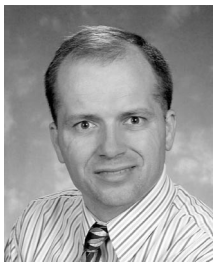

J. Mitch Wolff is an associate professor of mechanical engineering at Wright State University. He received his BS, MS, and PhD degrees in mechanical engineering from Purdue University in 1983, 1989, and 1995, respectively. He joined the Wright State faculty in September 1995 as an assistant professor. He is the author of over 35 technical papers and journal articles in the areas of propulsion, computational methods, and instrumentation. Dr. Wolff's current research interests include propulsion, turbomachinery, computational fluid dynamics, unsteady aerodynamics, instrumentation and flow measurement, and forced response. Dr. Wolff has been recognized with the SAE Ralph R. Teetor Educational Award, the ASEE Dow Outstanding New Educator Award, and the College of Engineering and Computer Science Teaching Effectiveness Award

in 1999. Dr. Wolff is a member of AIAA, SAE, ASEE and is the ASME student section faculty advisor.

Howard E. Jackson received the BS degree in physics from the University of Rochester, Rochester, New York, in 1965, and the PhD degree from Northwestern University, Evanston, Illinois, in 1971. He is presently Vice President for Research and University Dean of Advanced Studies, professor of physics, and Distinguished Teaching Professor, at University of Cincinnati, Cincinnati, Ohio. His current research interests include light scattering from solids, integrated optics utilizing both semiconductor and insulator materials, and near field scanning optical microscopy. His recent contributions have centered on understanding the electronic landscape of self-assembled quantum dots, the behavior of vertical cavity surface emitting lasers at high spatial resolution, photonic crystal behavior, and ion beam induced interdiffusion. Before joining the University of Cincinnati, he was associated with McMaster University, and the University of Toronto, Toronto, Ontario, Canada. He has been a visiting scientist at the Clarendon Laboratory, Oxford University, Oxford, England, and the University of Southampton, Southampton, England. Dr. Jackson is a member of Sigma Xi, the American Physical Society, and a Fellow of the Graduate School of the University of Cincinnati.

Joseph T. Boyd is currently professor of electrical and computer engineering at the University of Cincinnati. He received his PhD in electrical engineering from Ohio State University and then worked at Rockwell International and NCR before joining the University of Cincinnati. He is performing research in the area of integrated optoelectronics, having published and presented over 250 research papers. Working with a start-up company in Columbus, he received a 1996 R & D 100 Award. In 1994, he received the University of Cincinnati College of Engineering Outstanding Research Award. In 1991 he edited the IEEE reprint volume *Integrated Optics: Devices and Applications*. In 1988 he served as guest editor for a special issue on integrated optics of the *Journal of Lightwave Technology*. He has presented short-course tutorials on integrated photonics at technical meetings and industrial locations. He served six years as an elected officer of the IEEE Lasers and Electro-Optics Society.